GU J Sci 30(2): 123-132 (2017)

Gazi University

Journal of Science

http://dergipark.gov.tr/gujs

Shielding Effect Analysis of Various Configurations of the Square Patch Elements

Funda Ergün YARDIM[1,*], Nursel AKÇAM[1], Merve BAYRAKTAR[2]

[1]*Gazi University, Electrical-Electronics Engineering Department, TURKEY*
[2]*Ministry of Customs and Trade, Ankara, Turkey*

Article Info

Received: 01/06/2016
Revised: 23/10/2016
Accepted: 24/02/2017

Keywords

FSS
Green's Function
Method of Moments
Shielding effects
Patch elements

Abstract

In this study, a band-stop Frequency Selective Surface (FSS) was designed for a 5GHz frequency band. 2.4GHz, 3.6GHz, 4.9GHz, 5GHz and 5.9GHz frequency bands are the WLAN channels specified in IEEE 802.11 protocol. The devices are often used at 2.4GHz. But in most cases, this frequency cannot be used efficiently due to limited number of channels and excessive number of devices operating at this frequency. This drawback can be eliminated by using 5GHz frequency. Effective usage can be achieved because of the few numbers of equipments operating and many channels available in this frequency band. In this context, a FSS band stop filter was designed to prevent interference and block undesired waves within 5GHz frequency bands. Parameters such as FSS geometry, its period, the element type used, distance between the arrays, parameters of the medium, angle of incidence and polarization of the incident wave are important in FSS design. The shielding effect of the FSS in a 5GHz frequency band was examined by using Green's Functions and the Method of Moments (MoM). Square type patch elements were used in filter design. The FSS design was also tested under vertical polarization for various length and numbers of square patches. Best shielding effect was obtained under vertical polarization with $\theta = 0°$ and $\theta = 30°$ for a FSS design having 1 square patch. The FSS design for various numbers of square patch elements was also tested. Four different designs composed of 1, 4, 9 and 16 square patches acted as a stable filter in the 5GHz frequency band in vertical polarization for $\theta = 0°$ and $\varphi = 0°$. Undesired propagations were also low. This value indicates that the design is successful as a filter structure. The best shielding effectiveness was obtained for 1 square patch FSS design in vertical polarization at $\theta = 30°$. As the patch number increases some undesired propagations were observed between 11GHz and 12GHz. Especially for 9 square patch FSS design, at 11GHz frequency a 22dB undesired propagation was observed. This case shows that the FSS filters act also at 11GHz frequency which is undesirable.

1. INTRODUCTION

Electromagnetic waves have electric and magnetic field components and these waves propagate in space or material media. When an electromagnetic wave hits a surface some parts of the electromagnetic wave are reflected while some parts are transmitted depending on the electrical characteristic properties of the surface. The FSS structures change their reflection and transmission characteristics depending on the frequency of electromagnetic waves hitting the surface. These structures are periodic arrays of patches or openings placed on a dielectric medium as in Fig. 1 [1]. The FSS structures operate as a filter for electromagnetic waves passing desired frequencies while rejecting the others.

*Corresponding author, e-mail: fundaergun@gazi.edu.tr

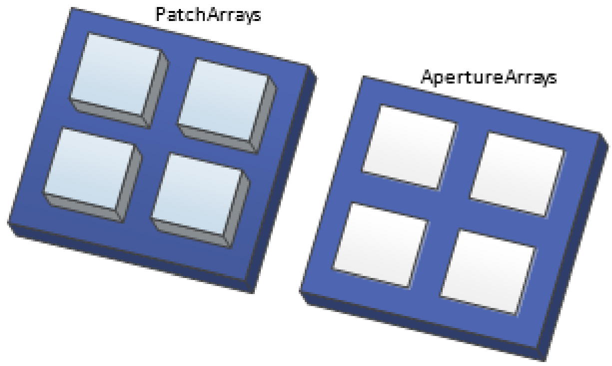

Figure 1.*Periodic FSS metallic patch and aperture arrays [1]*

FSS structures can be used in various applications such as, satellite systems [2], antennas and communication systems [3], Radio Frequency Identification – RFID [4], electromagnetic wave shielding and military [5], RADAR [6], civil applications [7] and, 3G and GSM networks [8].

MoM is one of the preferred methods that provides efficient and simple solutions to scattering analysis of FSS [9]. When an electromagnetic wave hits a FSS, the wave induces a current on the FSS surface and scattering occurs. When using MoM in frequency domain, the relation between the electric field and the induced current is obtained as a system of linear equations. The scattering and transmission coefficients can be obtained by solving these equation systems with the help of a computer. The scattering and transmission coefficients are used to express the current densities. By obtaining the electric field expression from the current densities, the shielding effect of FSS is calculated from the relation between the incident and transmitted electric fields [10,11].

In FSS design, parameters such as properties of the dielectric medium, the geometry of FSS, the period, patches and openings, type of the elements used, distance between the arrays, angle of incidence and polarization (Fig.2) are effective. These parameters determine the frequencies at which the FSS will transmit or reject the waves. In this study, square patch elements were used as they behave as more stable filters to changes in electromagnetic waves at angles of incidence [12].

In the literature, different methods such as genetic algorithm [13], artificial neural networks [14], V-dipole basis functions [15], Ewald Transform [16], Rao Wilton Glisson (RWG) basis functions [17], Maehly approximation [18] etc. are used in FSS analysis by adapting to the MoM. Also, Floquet modes and Green's functions [19] are widely used in the FSS analysis.

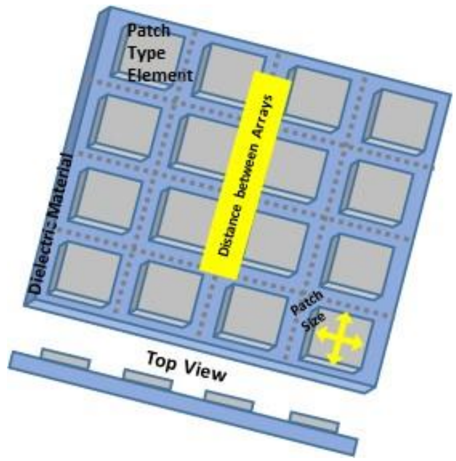

Figure 2. *Important FSS design parameters*

In section two of this study, design steps of the FSS structure, methods that were used for system solutions and the shielding effect of FSS are explained. In the third section, initially FSS and patch lengths were determined for best shielding effect. Some tests were conducted for different angle of incidence in vertical polarization by using patch elements of various numbers and lengths in order to examine the effect of FSS structure elements on shielding effect.

2. FORMULATION

The wave equation for the magnetic vector potential is given as follows [20]:

$$\nabla^2\vec{A} - \mu\varepsilon\frac{\partial^2\vec{A}}{\partial t^2} = -\mu\vec{J} \qquad (1)$$

Where ε is the electrical permittivity coefficient (F/m), μ isthe magnetic permeability coefficient (H/m), $\vec{J}$ is the volume current density per unit area (A/m2) and, $\vec{A}$ is the magnetic vector potential. Phasor scattered electric field caused by the magnetic vector potential is expressed as below [20].

$$\vec{E}^{\mathrm{scattered}}(r) = -j\omega\left[\vec{A}(r) + \frac{1}{k^2}\left(\nabla\left(\nabla.\vec{A}(r)\right)\right)\right] \qquad (2)$$

where, ω is the angular frequency and k is the wave number ($k = \omega\sqrt{\mu\varepsilon}$). When an electromagnetic wave hits the FSS surface, the relationship between the current induced on the conductive patch and the magnetic vector potential generated by this current at any point in the environment in which the FSS is placed can be expressed with Green's function as:

$$\vec{A}(r) = \int \vec{G}(r, r')\,\vec{J}(r')ds' \qquad (3)$$

where, r is the observation point and, r' is the source point. The solution of the Green's function for the magnetic vector potential is given as follows [21].

$$\vec{G} = \frac{e^{-jk|r-r'|}}{4\pi|r-r'|} \qquad (4)$$

Because the square-type patch element is used in FSS design; incident electric field and magnetic vector potential can be written in two dimensions. In this case, substituting x and y components of the incident electric field and expression of the magnetic vector potential into wave equation (Eq.(1)) yields the equation system in matrix form for components of $E_x^{incident}$ and $E_y^{incident}$ as below.

$$\begin{bmatrix} E_x^{incident} \\ E_y^{incident} \end{bmatrix} = -j\omega \begin{bmatrix} 1+\frac{1}{k^2}\frac{\partial^2}{\partial x^2} & \frac{1}{k^2}\frac{\partial^2}{\partial x \partial y} \\ \frac{1}{k^2}\frac{\partial^2}{\partial x \partial y} & 1+\frac{1}{k^2}\frac{\partial^2}{\partial y^2} \end{bmatrix} \begin{bmatrix} A_x \\ A_y \end{bmatrix} \tag{5}$$

The vector potential can be written as $\vec{A}(x,y)e^{j(a_m x + b_n y)}$ in two dimensions. Where, “m” and “n” show indices. a_m and b_n in the equation are the special frequencies that change depending on the square patch number and expressed as [10], [11]:

$$a_m = a_0 + \frac{2\pi}{a} m \tag{6}$$

$$b_n = b_0 + \frac{2\pi}{b} n \tag{7}$$

When Green’s Function is applied to the equation system obtained from electric field and magnetic vector potential expressions [10], [11]:

$$\begin{bmatrix} E_x(a_m, b_n) \\ E_y(a_m, b_n) \end{bmatrix} = -j\omega \begin{bmatrix} \frac{k^2 - a_m^2}{k^2} & \frac{-a_m b_n}{k^2} \\ \frac{-a_m b_n}{k^2} & \frac{k^2 - b_n^2}{k^2} \end{bmatrix} G(a_m, b_n) \begin{bmatrix} J_{x(a_m, b_n)} \\ J_{y(a_m, b_n)} \end{bmatrix} \tag{8}$$

By taking the Fourier Transform of Eq. (4), below expression is obtained.

$$G(a_m, b_n) = \frac{-j}{\sqrt{k^2 - a_m^2 - b_n^2}} \tag{9}$$

Linear equation system can be written as in its most general form by implementing Green’s function to Eq. (8)[10,11].

$$\begin{bmatrix} E_x(a_m, b_n) \\ E_y(a_m, b_n) \end{bmatrix} = -\frac{1}{2\omega\varepsilon} \sum_{m,n} \begin{bmatrix} \frac{k^2 - a_m^2}{\sqrt{k^2 - a_m^2 - b_n^2}} & \frac{-a_m b_n}{\sqrt{k^2 - a_m^2 - b_n^2}} \\ \frac{-a_m b_n}{\sqrt{k^2 - a_m^2 - b_n^2}} & \frac{k^2 - b_n^2}{\sqrt{k^2 - a_m^2 - b_n^2}} \end{bmatrix} \begin{bmatrix} J_{x(a_m, b_n)} \\ J_{y(a_m, b_n)} \end{bmatrix} e^{j(a_m x + b_n y)} \tag{10}$$

MoM has a wide-spread usage in electromagnetic problems containing integrals. Thus, MoM can be applied by inserting into the integral given in Eq. 11 where, $K(x, x')$ is the known Kernel function, $g(x)$ is the known source function and, $f(x)$ is the unknown functions [10], [11].

$$\int_a^b f(x') K(x, x') dx' = g(x) \tag{11}$$

In MoM, the unknown function $f(x)$ can be given as below where, a_n is the unknown coefficients and, $f_n(x)$ is the known base function.

$$f(x) = \sum_{n=1}^{N} a_n f_n(x) \tag{12}$$

As “L” is the integral operator, the general solution equation is obtained as follows by replacing MoM into integral given in the problem.

$$\sum_{n=1}^{N} a_n L\{f_n(x)\} = g(x) \tag{13}$$

The error function “W(x)” in MoM is given as in Eq. (14).

$$W(x) = \left[\sum_{n=1}^{N} a_n L\{f_n(x)\}\right] - g(x) \tag{14}$$

The MoM applied equation systems are:

$$[Z_{mn}][a_n] = [V_m] \tag{15}$$

$$[Z_{mn}] = \langle W_n | Lf_n \rangle \tag{16}$$

$$[V_m] = \langle W_m | g \rangle \tag{17}$$

In MoM, different types of functions are used in order to define the error and base functions. Generally, Dirac Delta Functions and Galerkin Method are used for error functions, while whole region or sub region base functions are used for base functions [20]. If the problem type is linear or regular, using whole region base functions will provide more easy and rapid solutions. For structures having different geometries, sub region base functions yield better results.

In this study, the FSS problem type is a regular square patch so, whole region base functions were used in problem solving. For error functions, Galerkin Method was used and, the following equation system was defined.

$$W_m = f_n \tag{18}$$

$$[Z_{mn}] = \langle f_m | Lf_n \rangle \tag{19}$$

$$[V_m] = \langle f_m | g \rangle \tag{20}$$

After defining error and base functions, by applying MoM, for the equations Z_{mn}, a_n, and V_m (Eq.(16 – 17)), Ax = b linear equation system (Eq.(15)) is obtained. By using Galerkin Method and replacing all data, Ax = b linear equation system is obtained in most general form as below [10,11].

$$\begin{bmatrix} \langle f_1 | Lf_1 \rangle & \cdots & \langle f_1 | Lf_n \rangle \\ \vdots & \ddots & \vdots \\ \langle f_m | Lf_1 \rangle & \cdots & \langle f_m | Lf_n \rangle \end{bmatrix} \begin{bmatrix} a_1 \\ \vdots \\ a_n \end{bmatrix} = \begin{bmatrix} \langle f_1 | g \rangle \\ \vdots \\ \langle f_m | g \rangle \end{bmatrix} \tag{21}$$

3. SIMULATION RESULTS

The electromagnetic interception process to reduce the leakage and undesired fields is called as shielding and, the Shielding Effectiveness (SE) can be expressed in decibels (dB) as follows:

$$SE_{dB} = 20 \log_{10} \frac{E^{incident}}{E^{transmitted}} \tag{22}$$

The shielding effectiveness of FSS depends on the element types used, size of the FSS and patches, angle of incidence and polarization. Especially element types used is FSS is important in the FSS design. Each element type has its own characteristic, therefore in the FSS design it is very important to select the element type according to the type of the problem. The designed FSS in this study is desired to be a stable band stop structure in 5 GHz. Square patch elements were used in this study because they are more stable to variations of angle of incidence.

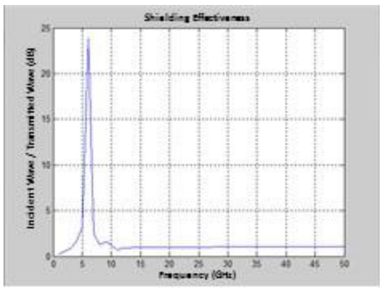

(a)

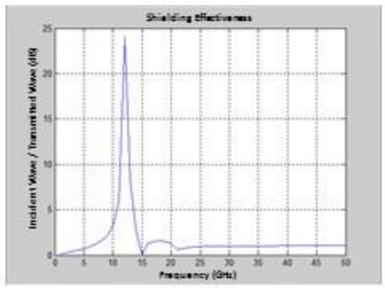

(b)

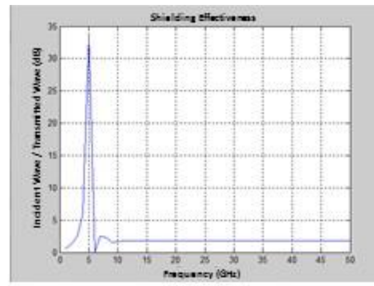

(c)

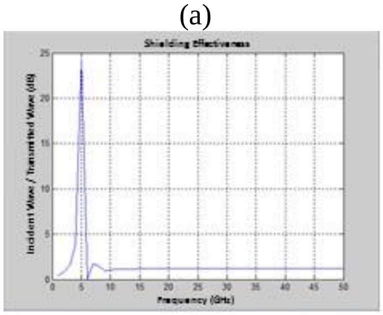

(d)

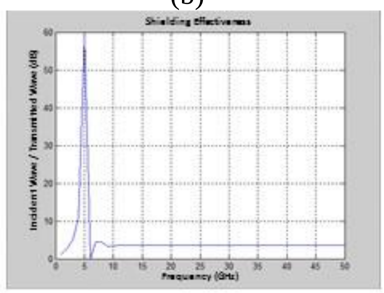

(e)

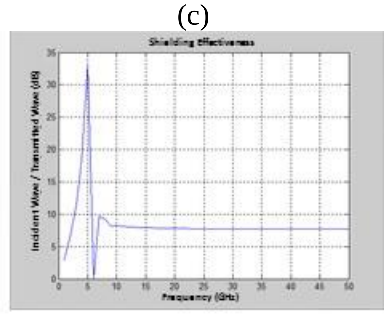

(f)

Figure 3. *FSS shielding effectiveness (a) FSS: 20mm, patch:1mm (b) FSS:40mm, patch:1mm (c) FSS:50mm, patch:10mm (d) FSS:50mm, patch:20mm (e) FSS:50mm, patch:30mm (f) FSS: 50mm, patch:40mm [10], [11]*

After determining the FSS element type, the patch size should be defined. Tests have been conducted for different FSS and patch sizes. The best shielding effectiveness was obtained for FSS length: 50mm and patch length: 30mm (Fig. 3) for 5GHz [10,11].

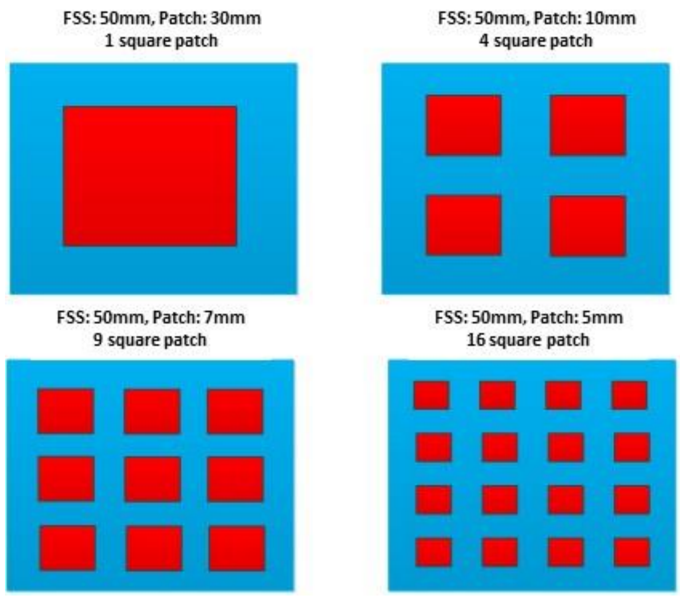

Figure 4. *FSS design for different square patch numbers*

Shielding effectiveness was tested for different angles of incidence by using various patch numbers and sizes (Fig. 4). The test results were given in Fig 5 to Fig. 12. As seen from Fig 5 to Fig.12, the best shielding effectiveness was obtained for 1 square patch FSS design in vertical polarization for $\theta = 0°$ and $\theta = 30°$. As the patch number increases and the angle of incidence changes, some undesired propagations were observed between 11GHz and 12GHz. At 11GHz a 22dB undesired propagation was detected for 9 square patch FSS design.

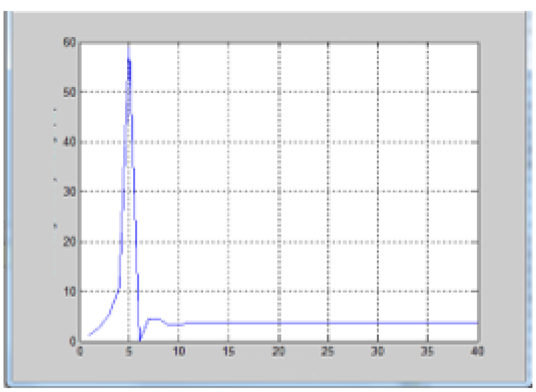

Figure 5. *Shielding effectiveness for 1 square patch FSS design in vertical polarization for θ=0° with parameters FSS:50mm, patch:30mm*

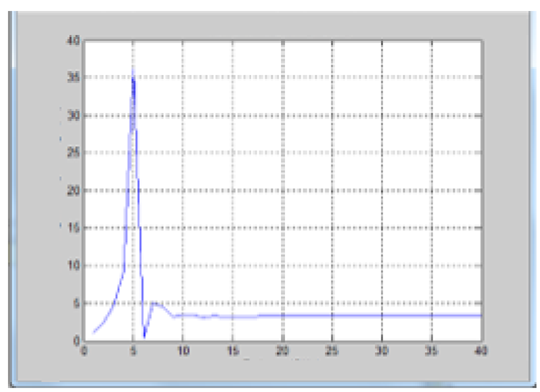

Figure 6. *Shielding effectiveness for 4 square patch FSS design in vertical polarization for θ=0° with parameters FSS:50mm, patch:10mm*

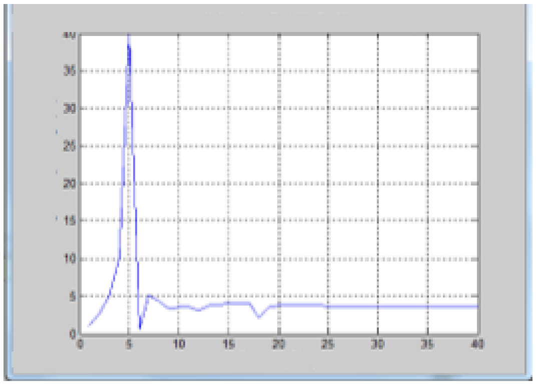

Figure 7. *Shielding effectiveness for 9 square patch FSS design in vertical polarization for θ=0° with parameters FSS:50mm, patch: mm*

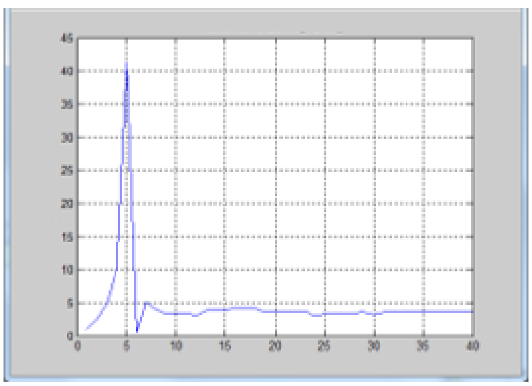

Figure 8. *Shielding effectiveness for 16 square patch FSS design in vertical polarization for θ=0° with parameters FSS:50mm, patch:5mm*

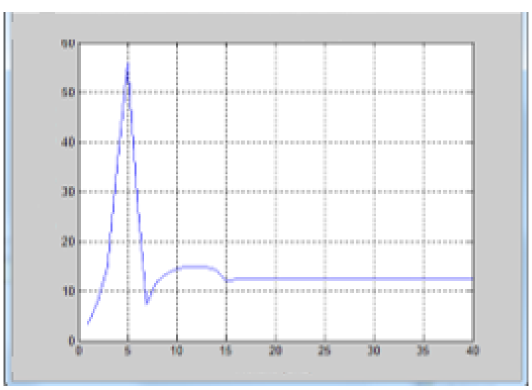

Figure 9. *Shielding effectiveness for 1 square patch FSS design in vertical polarization for θ=30° with parameters FSS:50mm, patch:30 mm*

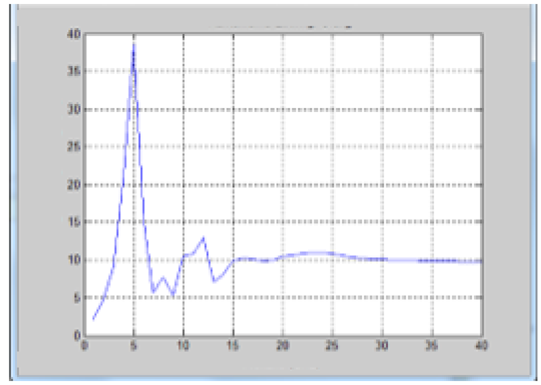

Figure 10. *Shielding effectiveness for 4 square patch FSS design in vertical polarization for θ=30° with parameters FSS:50mm, patch:10mm*

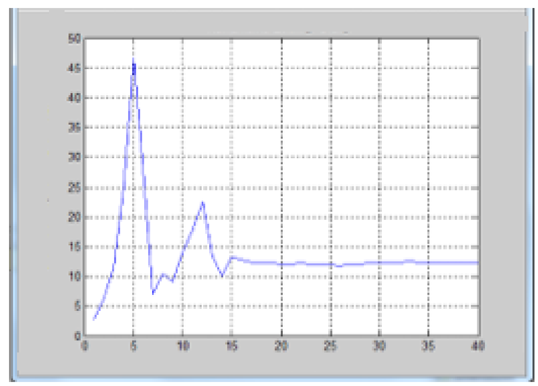

Figure 11. *Shielding effectiveness for 9 square patch FSS design in vertical polarization for θ=30° with parameters FSS:50mm, patch:7mm*

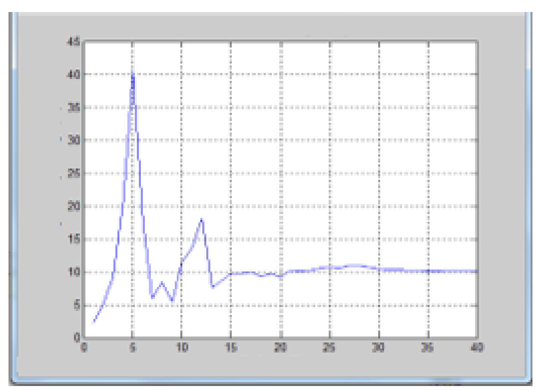

Figure 12. *Shielding effectiveness for 16 square patch FSS design in vertical polarization for θ=30° with parameters FSS:50mm, patch:5mm*

4. CONCLUSION

In this study a band stop FSS design was introduced to eliminate the interference and undesired waves at 5GHz frequency band. Square type patch elements were used because of their stable shielding effectiveness and filter response. Also square patch type elements gave more uniform responses to changes in the angle of incidence and polarization of electromagnetic waves. The FSS and patch sizes were determined in order to design a band stop filter in 5GHz. The best shielding effectiveness was obtained for FSS length: 50mm and patch length: 30mm (Fig. 3) for 5GHz frequency band [10,11].

The FSS design for various numbers of square patch elements was also tested. Four different designs composed of 1, 4, 9 and 16 square patches acted as a stable filter in the 5GHz frequency band in vertical polarization for $\theta = 0°$ and $\varphi = 0°$. Undesired propagations were also low. This value indicates that the design is successful as a filter structure. The best shielding effectiveness was obtained for 1 square patch FSS design in vertical polarization at $\theta = 30°$. As the patch number increases some undesired propagations were observed between 11GHz and 12GHz.Especially for 9 square patch FSS design, at 11 GHz frequency a 22dB undesired propagation was observed. This case shows that the FSS filters act also at 11 GHz frequency which is undesirable.

5. REFERENCES

[1] Gökçen, A., Ünal, E., Kutlu, Y., "Shielding Effectiveness of Periodic Square and Circle Shaped Frequency Selective Surface Placed on Dielectric Media for the 1800 MHz", İTUSEM, (2005).

[2] Maini, Agrawal, V., "Satellite Technology: Principles and Applications", John Wiley & Sons, New York City/United States, 694(2011).

[3] Capolino, F., "Applications of Metamaterials", CRC Press, London/England, 762(2009).

[4] Shen, Z., "Millimeter Wave Imaging Technologies for Plasma Diagnostics on Superconducting Tokomak Machines", Pro-Quest, Michigan/United States, 197(2007).

[5] Elbert, B. R., "The Satellite Communication Applications Handbook", Artech House, London/England, 551(2004).

[6] Balanis, C. A., "Modern Antenna Handbook", John Wiley & Sons, New York City/United States, 1074 (2011).

[7] Wu, T. K., "Frequency Selective Surface and Grid Array", Wiley, New York City/United States, 331(1995).

[8] Subrt, L., Grace, D. and Pechac, P., "Controlling the Short-Range Propagation Environment Using Active Frequency Selective Surfaces", Radio Engineering, 19(4): 610-617, (2010).

[9] Celozzi, S., Araneo, R. and Lovat, G., "Electromagnetic Shielding", John Wiley & Sons, New York City/United States, 385 (2008).

[10] Bayraktar, İ. M., "Frequency Selective Surface Applications on CPU and GPU", MSc. Thesis, Gazi University, Graduate School of Natural and Applied Sciences, Ankara, 43-52 (2015).

[11] Bayraktar, I.M., AKÇAM, N., YARDIM, F.E., "Band Stop Frequency Selective Surface Design For WLAN Channel", 3trd International Symposium on Innovative Technologies in Engineering and Science (ISITES 2015), Valencia/Spain, 1659-1668, (2015).

[12] Munk, B. A., "Frequency Selective Surfaces: Theory and Design", John Wiley & Sons, New York City/United States (2000).

[13] Lanuzza, L., Monorchio, A. and Manara, G., "Synthesis of High-Impedance FSSs Using Genetic Algorithms", IEEE, 364-637(2002).

[14] Paulo, H., Silva, F., Lacaouth, P., Fontgalland, G., Campos, A. and Assunçao, A., "Design of Frequency Selective Surfaces Using a Novel MoM-ANN-GA Technique", IEEE, 275-279 (2007).

[15] Poulsen, S., "Scattering From Frequency Selective Surfaces: An Efficient Set of V-Dipole Basis Functions", IEEE, 540-548(2003).

[16] Bringuier, J. N. and Mittra, R., "Efficient Analysis of Frequency Selective Surfaces Using the Ewald Transform", IEEE, 2645-2648 (2011).

[17] Zhuang, W., Fan, Z. H., Ding, D. Z. and Chen, R.S., "An Efficient Technique for Analysis of Frequency Selective Surface in Spectral Domain with RWG Basis Functions", IEEE, 224-226 (2008).

[18] Ma, X., Wan, G. B. and Wan, W., "Efficient Analysis of FSS Using the MoM-based Maehly Approximation", IEEE, 21-24 (2011).

[19] Weile, D. S., "Analysis of Frequency Selective Surfaces Through the Blazing Onset Using Rational Krylov Model-Order Reduction and Woodbury Singularity Extraction", IEEE, 49(10):1470-1478, (2001).

[20] Balanis, C. A., "Advanced Engineering Electromagnetics", John Wiley & Sons, New York City/United States, 670-743(1989).

[21] Akira, I., "Electromagnetic Wave Propagation, Radiation and Scattering", Prentice Hall, New Jersey /United States, (1991).